Radio frequency electrode system for optical lesion size estimation in functional neurosurgery

Johan Antonsson
Linköpings Universitet
Department of Biomedical Engineering
Sweden

Ola Eriksson
Linköpings Universitet
Department of Biomedical Engineering
Sweden
and
Elekta Instrument AB
Sweden

Karin Wårdell
Linköpings Universitet
Department of Biomedical Engineering
Sweden

Abstract. Radiofrequency (RF) lesioning in the human brain is one possible surgical therapy for severe pain as well as movement disorders. One obstacle for a safer lesioning procedure is the lack of size monitoring. The aim of this study was to investigate if changes in laser Doppler or intensity signals could be used as markers for size estimation during experimental RF lesioning. A 2 mm in diameter monopolar RF electrode was equipped with optical fibers and connected to a digital laser Doppler system. The optical RF electrode's performance was equal to a standard RF electrode with the same dimensions. An albumin solution with scatterers was used to evaluate the intensity and laser Doppler signal changes during lesioning at 70, 80, and 90 °C. Significant signal changes were found for these three different clot sizes, represented by the temperatures ($p<0.05$, $n=10$). The volume, width, and length of the created coagulations were correlated to the intensity signal changes ($r=0.88$, $n=30$, $p<0.0001$) and to the perfusion signal changes ($r=0.81$, $n=30$, $p<0.0001$). Both static and Doppler-shifted light can be used to follow the lesioning procedure as well as being used for lesion size estimation during experimental RF lesioning. [DOI: 10.1117/1.1924615]

Keywords: radiofrequency; functional neurosurgery; lesion size; laser Doppler; brain electrodes.

Paper 04010 received Jan. 30 2004; revised manuscript received Nov. 17, 2004; accepted for publication Feb. 11, 2005; published online May 24, 2005.

1 Introduction

Radio frequency (RF) lesioning has been used in functional neurosurgery since the 1950s.[1] With this interventional technique, permanent cell damage is achieved and it must therefore be performed with high accuracy and precision. Clinical applications are, e.g., symptom relief of movement disorders such as Parkinson's disease[2–5] and the reduction of severe chronic pain.[6] During RF lesioning, Joule heating of the tissue in the proximity of the electrode tip creates the coagulation. To achieve an optimal outcome of the intervention, the localization of the target and the lesion's size and shape must be considered. In the last few years, improvement of target localization has been achieved by the implementation of increased resolution in different imaging modalities such as magnetic resonance imaging (MRI) and computer tomography (CT) and their integration in preplanning surgical systems.[7] Furthermore, microelectrode mapping of the neurophysiological activity[8,9] together with an increased knowledge of the pathophysiology of the basal ganglia[10] are also used to improve target localization.

Knowledge of the lesion size and shape is crucial to the surgical outcome. If the lesion is too large irreversible complications might occur and if it is too small the expected effect may be lost. Previous investigations have shown that the size and shape is influenced by parameters such as electrode configuration and temperature settings.[11] A linear relation between target temperature and lesion size has been found by using transparent homogenous albumin as a test solution in combination with a computer-assisted video system for documentation of the clot length, width, volume, and shape.[11,12] Furthermore, the same electrode tests showed a high correlation with stereotactic thalamic lesions in the pig brain evaluated by MRI and postmortem histology sectioning.[13] In living tissue, however, other parameters such as tissue type and blood perfusion in the target and its closest surroundings can also influence the size and shape.[14] Up to now, the lesioning process has been clinically studied by observing the patient's reactions during the surgical procedure as well as postoperatively by investigating the lesion's localization and size using MRI or CT.[15] Currently, there are no methods that can record the lesioning process intracranially parallel to the coagulation development with the necessary image resolution and scanning speed. The first part during RF surgery is most important to monitor, due to the major coagulation development is occurring during the first 10–20 s of lesioning. Image modalities such as intraoperative MRI, CT, or ultrasound is currently not appropriate for lesion size estimation during stereotactic RF lesioning, due to the relative low image resolution or scanning

Address all correspondence to Johan Antonsson, Linköpings Universitet, Department of Biomedical Engineering, 581 85 Linköping, Sweden. Tel: +046 13 222456; Fax: +046 13 101902; E-mail: johan@imt.liu.se

1083-3668/2005/$22.00 © 2005 SPIE

speed,[16–18] however, there is a vast amount of research ongoing to improve these imaging techniques.

In order to monitor the optical changes in the surrounding media during lesioning, a RF electrode system was modified. Optical fibers were inserted along the electrode to deliver and collect backscattered laser light from the surrounding media. The backscattered photons were converted to an electrical signal, which was processed in order to detect unshifted and Doppler-shifted light before, during and after a coagulation process. The aim of this study was to evaluate the developed system's performance by using an *in vitro* model and to investigate if optical variations could be used as markers for size estimation during experimental RF lesioning.

2 Optical RF Electrode System

A schematic overview of the optical RF lesioning system is presented in Fig. 1(a). It comprises an optical RF electrode, Leksell® Neuro Generator (LNG) (model 30-1, Elekta Instrument AB, Sweden), a low-power He–Ne laser at 633 nm, laser Doppler detection hardware (photodetector with filters), analog/digital converter and a computer for processing and presentation of collected data. The system has five temporal output signals: temperature, power, and impedance from the LNG, perfusion, and total backscattered light intensity from the laser Doppler unit.

2.1 *Optical RF Electrode*

A monopolar optical RF electrode was designed following the same construction principle as a 2 mm in diameter standard monopolar electrode with an unisolated tip length of 4 mm (Elekta Instrument AB, Sweden). A bundle of 230 μm step index glass fibers was inserted inside the electrode to the tip. The light illuminates the measured volume perpendicular to the electrode tip via a transparent window, which also serves as isolation between the tip and shaft.

2.2 *Signal Processing*

Laser Doppler flowmetry is a well established method that measures microvascular blood perfusion.[19,20] The method is based on the detection of backscattered laser light from a small tissue volume containing both Doppler-shifted and unshifted scattered photons. A perfusion value, defined as the mean concentration of moving red blood cells times their mean velocity, is estimated via digital signal processing according to Eq. (1)[21]:

$$\text{Perfusion} = \frac{1}{\langle \text{DC}[N_{\text{DC}}] \rangle^2} \sum_{\omega=F1}^{F2} \omega \cdot P_{\text{AC[Nac]}}[\omega] - f_{\text{Noise}}[\langle \text{DC}[N_{\text{DC}}] \rangle]. \quad (1)$$

In Eq. (1), AC corresponds to the detected unprocessed frequency shifted signal and DC to the total backscattered light intensity. The DC value is an average calculated over N_{DC} samples. $P_{\text{AC[Nac]}}[\omega]$ is an estimate of the power spectral density calculated from N_{ac} points of the sampled AC signal. The function $f_{\text{Noise}}[\langle \text{DC}[N_{\text{DC}}] \rangle]$ is a linear noise function. F_1 and F_2 are the lower and upper cutoff frequencies, in this system set to a bandwidth corresponding to 20 Hz and 12 kHz. The analog AC and DC signals were sampled with a sampling frequency set to 25 kHz (6070 DAQ Pad, National Instruments, Inc. USA) using LabView® (National Instruments Inc., USA). Routines for offline analysis and processing of collected signals were developed in MATLAB® (The Mathworks Inc., USA).

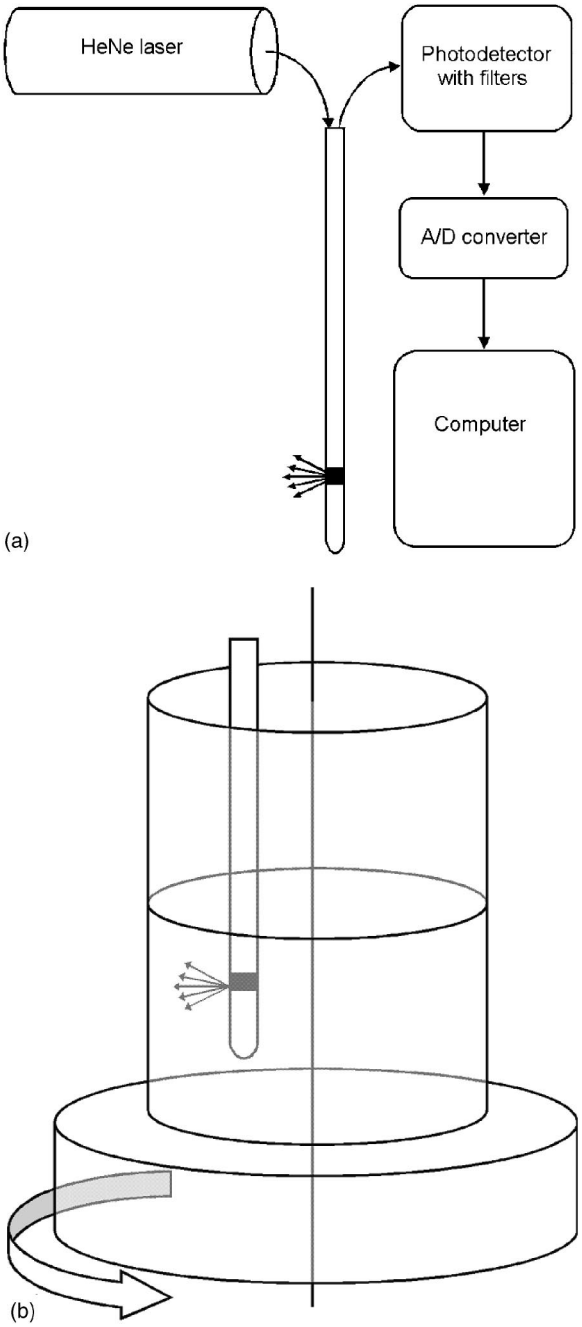

Fig. 1 System overview (a), flow model with the revolving disk (b).

2.3 *Evaluation of the Laser Doppler Unit*

Measurements were conducted with the RF electrode in a Delrin® piece of plastic with drilled holes of diameters between 2 and 12 mm, in order to investigate the system capability of detecting nonshifted photons. The optical RF electrode system's ability to detect Doppler-shifted light and the system linearity were tested in a flow model. A bowl with a

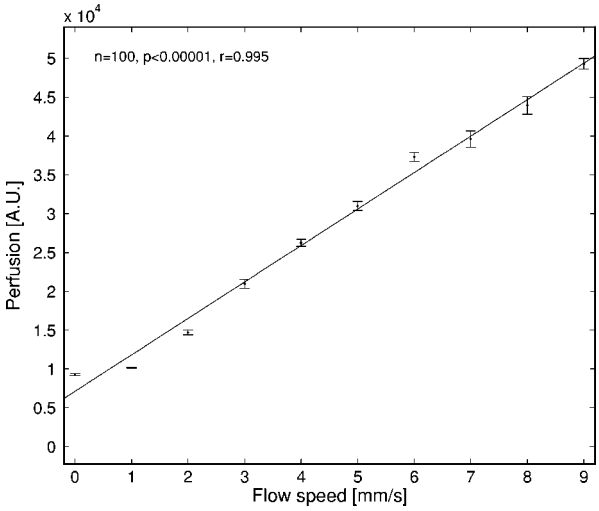

Fig. 2 Linearity of the optical RF lesioning system.

2% microsphere diluted albumin solution was placed on top of a revolving disk, Fig. 1(b). The optical electrode was placed into the solution at a fixed distance from the rotational center. Via the angular frequency and electrode distance from the rotational center, the flow speed at the electrode tip was calculated. By changing the angular frequency, flow speeds between 0 and 9 mm/s were achieved. The solution passed perpendicularly to the electrode tip and the light from the electrode was thus transmitted into the moving solution. A fraction of the backscattered photons from the moving particles was detected, which gave rise to the perfusion signal. The calculated perfusion signals showed a linear relationship with the flow speed between 0 and 9 mm/s ($r=0.995$, $p<0.00001$, $n=100$), Fig. 2.

3 Experimental Setup

3.1 *Video System and Test Solutions*

A previously developed computer-assisted video system[11,12] was used to evaluate the RF electrode system performance. The system uses two perpendicular JPEG images taken with a digital camera (Canon powershot s10) to calculate the height, width and volume of the coagulations. The JPEG images in this study were captured in a transparent saline solution and the electrode shaft diameter was used as a size reference according to previously developed methods.[11]

The test solution contained bovine albumin fraction V (Biochemical Ltd., UK) diluted in saline (9 mg/mL). This solution has previously been used to investigate the size of generated protein clots.[11] To simulate microvascular perfusion during coagulation of the albumin solution, glass microspheres at 11 μm diameter (Potters Ltd., USA) were added to a concentration of 2%, mimicking red blood cells.

3.2 *Coagulation Evaluation and Optical Markers*

To study the developed RF electrodes capability of creating equally sized coagulations as a standard electrode, and to investigate the relationship between the created coagulations and the changes in perfusion and intensity signals, two separate set of experiments were performed. The first set of coagulations was created in the standard albumin solution with both the optical RF electrode and a comparable standard 2 mm in diameter RF electrode. The albumin solution was heated to 37 °C and lesions were created at target temperatures of 70, 80, and 90 °C for 60 s. In the second experiment, another set of coagulations was created with the optical RF electrode in a 24 °C microsphere diluted albumin solution. To simulate blood flow the bowl with the microsphere solution was put on top of the revolving disk, Fig. 1(b). The optical RF electrode was then put into the solution at a distance of 10 mm from the rotational center. The angular frequency of the disk was measured and the flow speed of the solution passing the electrode tip was estimated to 1 mm/s. The optical measurements were started 10 s before the lesioning process and stopped 10 s after. The time and temperature settings were again 60 s at 70, 80, and 90 °C. For each temperature and electrode configuration, ten separate lesions were created. In total of the two experiments 60 lesions were created in standard albumin and 30 lesions in the microsphere diluted solution.

3.3 *Data Analysis*

The mean and standard deviations (m±s.d.) of the clot volume, width and length were calculated for all temperature, electrode and albumin solution configurations.

The mean value of the DC and perfusion signal 10 s before (DC_{Pre},$Perf_{Pre}$) and 10 s after (DC_{Post},$Perf_{Post}$) the coagulation was calculated. To test the significance of the changes in DC and perfusion signals before and after coagulation a paired two-tailed Student t test was used, where $p<0.05$ was considered significant.

The relative changes of the signals pre- and postlesioning were expressed in quotients. The DC_{Pre}, DC_{Post}, and $Perf_{Pre}$, $Perf_{Post}$ were used to calculate two different quotients (Q_{DC} and Q_{Perf}) according to Eqs. [2(a)–2(b)]:

$$Q_{DC}=\frac{DC_{Post}}{DC_{Pre}}, \tag{2a}$$

$$Q_{Perf}=\frac{Perf_{Post}}{Perf_{Pre}}. \tag{2b}$$

The calculated signal changes for the temperatures of 70, 80, and 90 °C were grouped together. The differences between these groups (70, 80, and 90 °C) were tested with a Kruskal–Wallis test (a nonparametric version of the one-way analysis of variance test), where $p<0.0005$ was considered significant. The association between signal changes and coagulation sizes (length, width, and volume) was investigated by calculating a linear regression model.

4 Results

The developed optical RF electrode creates coagulations with similar size and shape as the standard RF electrode. An example of the coagulation shape at 80 °C in the standard albumin solution with the two electrodes is presented in Fig. 3. The calculated volume, width and length for the lesions created with the two RF electrodes are presented in Table 1.

Typical signal patterns of a coagulation procedure in the microsphere solution with a heating period of 60 s and a rest-

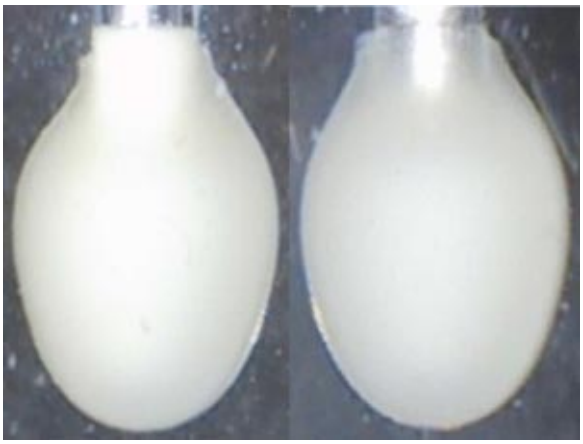

Fig. 3 Example of two 80 °C lesions created in a standard albumin solution with the optical electrode (a) and the standard electrode (b).

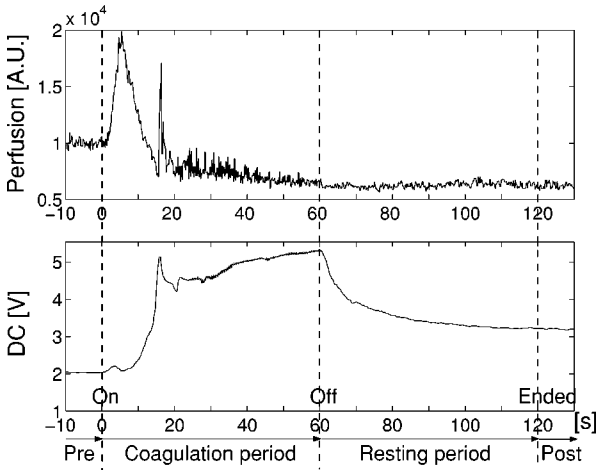

Fig. 4 An example of boiling during coagulation at 90 °C, the signal above is perfusion and the signal below is DC.

ing period of additional 60 s are presented in Fig. 4. A 10 s base line recording precedes the lesioning. After initiation of the coagulation the DC and perfusion signals display a steep increase, with a perfusion peak after 5 s and a slower DC increase rate after 15 s. The perfusion signal decreases as soon as the albumin protein begins to coagulate but the DC signal flattens out. In this example, a second pronounced peak is seen in the perfusion signal after 18 s. This peak is caused by boiling, often occurring during coagulation at high temperatures (here 90 °C) and is manifested as a bleb formation of the clot.[11] The DC signal is only slightly influenced by the boiling of the albumin solution. When the LNG is turned off (marked ended at the 120 s marker), both the DC and perfusion signals reach a stable but different level, compared to the base line.

An example of the recorded DC and perfusion signal changes during coagulations at 70, 80, and 90 °C is shown in Fig. 5. To emphasize the signal changes pre- and postcoagulation, the DC and perfusion signals were normalized to their corresponding base lines. After a short heating period, the perfusion signal for all three temperatures rose to a high peak value, Fig. 5(a). When the LNG procedure was ended three different stable perfusion levels were detected with all values situated below the base line. Larger clots (higher temperature) showed lower perfusion values, Fig. 5(a). The changes in perfusion levels before and after coagulation were significant for all three of the temperature settings ($p<0.001,\ n=10$). The coagulation development can also be seen in the increased DC signals Fig. 5(b). When the LNG was turned off three different stable DC levels were detected with all values situated above the base line. Distinct signal levels were found between the 70, 80, and 90 °C clots. Larger clots (higher temperature) showed larger DC levels. The DC signal changes before and after lesioning were significant for all three temperatures ($p<0.05$, $n=10$ for 70 °C and $p<0.001$, $n=10$ for both 80 and 90 °C).

The calculated signal changes, according to Eqs. [2(a)–2(b)] with corresponding standard deviations, were plotted against the created three different volumes in Fig. 6. The changes for the DC values are presented as values above 100% due to the increase of the DC signal during coagulation. There was a high significance ($p<0.0005,\ n=30$) between the different signal changes for both the DC and perfusion signals for all tested temperatures.

A linear relationship between the measured coagulation sizes and the calculated signal changes was found with a linear regression model in the albumin solution with microspheres. The correlation between Q_{DC} and volume, length, and width of the clots, respectively, was at least $r=0.88$ ($p<0.0001,\ n=30$). Also Q_{perf} was correlated with the clot volume, length, and width. The correlation coefficient was at least $r=0.81$ ($p<0.0001,\ n=30$).

5 Discussion

In this study, a system for the investigation of optical measurements during radio frequency thermolesioning has been

Table 1 Mean values and standard deviations ($n=10$) of volume, width, and length, of lesions created with the standard and optical electrode in standard albumin, at 70, 80, and 90 °C.

	Volume mm^3±std		Length mm±std		Width mm±std	
	Standard	Optical	Standard	Optical	Standard	Optical
70 °C	58.2± 2.7	51.7± 3.6	5.9±0.1	5.5±0.2	4.3±0.1	4.2±0.1
80 °C	89.6± 4.0	90.2± 4.9	7.0±0.1	6.7±0.2	4.9±0.1	5.0±0.1
90 °C	164.0±26.3	157.6±11.9	8.5±0.6	8.4±0.3	6.1±0.3	6.0±0.1

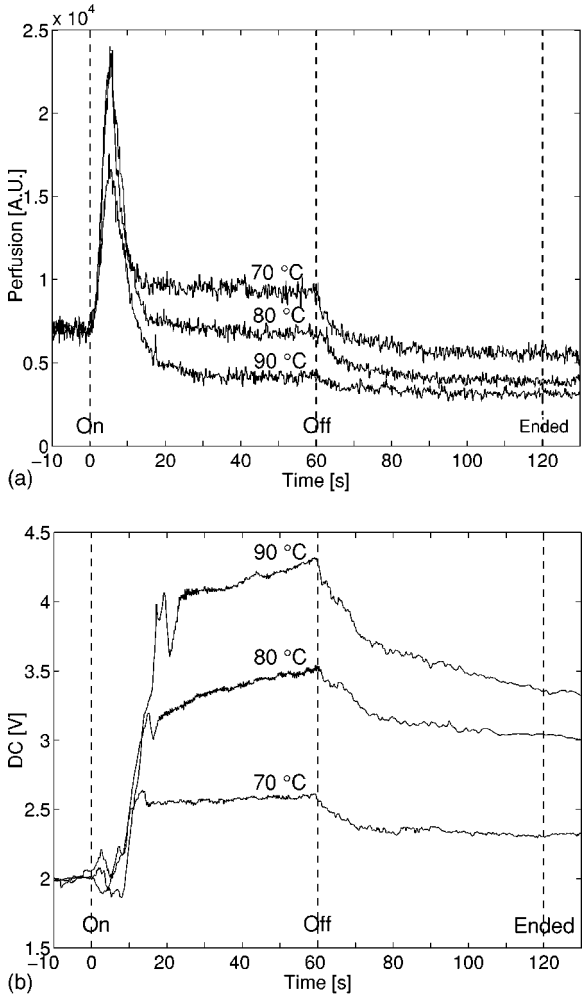

Fig. 5 An example of perfusion (a) and DC (b) signals during lesioning at temperatures of 70, 80, and 90 °C.

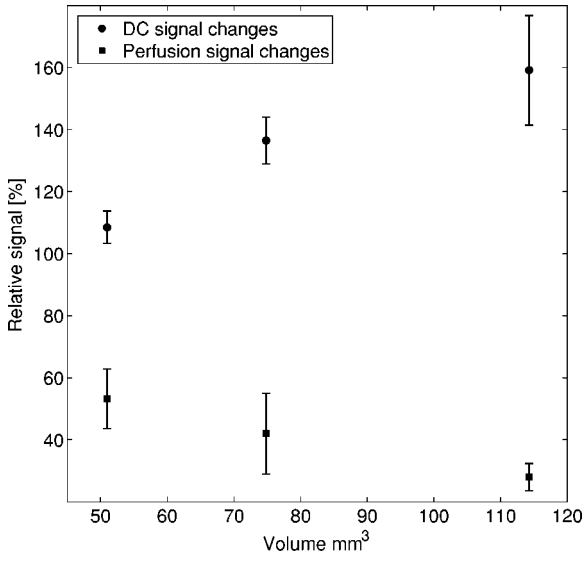

Fig. 6 Relative changes for DC and perfusion signals at 70, 80, and 90 °C.

presented and evaluated. A brain lesioning electrode with integrated optical fibers inserted towards an optical window at the electrode tip, was developed. The changes in both static and Doppler-shifted light in the vicinity of the tip during lesioning were investigated. These experiments show that perfusion and DC changes can be used as markers for lesion size estimation *in vitro*.

The perfusion signal, originates from the backscattered Doppler-shifted light processed according to the laser Doppler theory, and is proportional to the average number of moving scatterers times their mean velocity in the sampling volume.[19,20] During coagulation of the tissue (here modeled as albumin with moving microspheres) the number of moving scatterers close to the electrode tip is reduced when the clot size is increased. An inverse relationship between the Doppler signal and clot size is thus expected. The sampling depth, however, is one limiting factor. Previous studies have shown that a 90 °C clot created with a 2 mm in diameter electrode does not expand more than 2 mm from the electrode surface,[13] which is considered to be within reach of the sampling depth of laser Doppler signals in the brain.[22,23] In addition, Giller and colleagues[24,25] have performed both phantom studies and Monte Carlo simulations in order to investigate the ''look-ahead distance'' for an near infrared probe used in diffuse reflectance spectroscopy. Depending on the optical scattering and absorption coefficients of the media and the used equipment the look-ahead distance varied between 1 and 3 mm. These simulations support our results of DC measurements within a 2 mm distance light source to coagulation border. A way of increasing the sampling depth in our application may be to change the used light source to a longer wavelength.

Electrical properties (resistance, delivered current, etc.) for both electrodes used in the first part of the study were measured and had the same values. The comparison between protein clots generated in 37 °C albumin without scatterers by a regular brain lesioning RF electrode and the optical RF electrode showed practically no difference in size and shape. The standard deviation of the volume, width, and length within one temperature setting was small for both electrodes, which implies good reproducibility.

The developed albumin model with microspheres has some features that have to be taken into consideration. A 24 °C microsphere diluted albumin solution was used in the rotating disk setup. The change in temperature between the experiments was performed due to difficulties to heat the solution without causing turbulent flow in the liquid. An agiated solution has a forced convective cooling at the electrode tip which results in slightly smaller coagulations, however, the investigated signal changes were compared to the created coagulations in the model and not the absolute sizes created in the stationary 37 °C experiment. A limitation of the model was a sediment effect of the microspheres due to their low buoyancy, which could affect the Doppler part of the measurements with a slightly increased perfusion base line level. For the experiments performed, the model was found to be adequate to monitor perfusion and DC changes around the electrode tip during coagulation. When the albumin solution starts to coagulate two distinct effects were expected and did occur. The optical reflectivity increases and the perfusion decreases, due to the reduced amount of freely moving scatterers close to the electrode tip. A characteristic signal pattern and a signifi-

cant change of signal levels pre- and postlesioning between 70, 80, and 90 °C were found. The correlation between lesion size and DC signal changes were slightly higher than for perfusion signals. This implies that the DC signal might be a better choice than the perfusion signal for estimating lesion sizes *in vitro*. But *in vivo* in a more turbid media, this result might be different. The DC and perfusion signal represents different properties in the measured volume and is therefore both important.

The presented system is currently evaluated *in vivo* using an animal model. The next step in the development towards a system for on-line estimation of lesion size after the animal evaluation is adaptation of the system for human use and clinical evaluation. Our hope is that the use of an optical RF electrode will become a valuable tool during functional neurosurgery, both for monitoring the lesion development and to give an indication of the actual created lesion size.

Acknowledgments

The authors would like to thank Research Engineer Håkan Rohman for building the electrode and Elekta Instrument AB, Sweden. This study was supported by the Swedish National Competence Center for Non-invasive Measurement (NIMED).

References

1. L. Leksell, ''A stereotaxic apparatus for intracerebral surgery,'' *Acta Chir. Scand.* **99**, 229–233 (1949).
2. R. M. de Bie, P. R. Schuurman, D. A. Bosch, R. J. de Haan, B. Schmand, and J. D. Speelman, ''Outcome of unilateral pallidotomy in advanced Parkinson's disease: cohort study of 32 patients,'' *J. Neurol., Neurosurg. Psychiatry* **71**(3), 375–382 (2001).
3. K. J. Burchiel, ''Thalamotomy for movement disorders,'' *Neurosurg Clin. N. Am.* **6**(1), 55–71 (1995).
4. D. Yoshor, W. J. Hamilton, W. Ondo, J. Jankovic, and R. G. Grossman, ''Comparison of thalamotomy and pallidotomy for the treatment of dystonia,'' *Neurosurgery* **48**(4), 818–824 (2001); **48**, 824–826 (2001).
5. R. M. de Bie, R. J. de Haan, P. C. Nijssen, A. W. Rutgers, G. N. Beute, D. A. Bosch, R. Haaxma, B. Schmand, P. R. Schuurman, M. J. Staal, and J. D. Speelman, ''Unilateral pallidotomy in Parkinson's disease: a randomised, single-blind, multicentre trial,'' *Lancet* **354**(9191), 1665–1669 (1999).
6. M. I. Hariz and A. T. Bergenheim, ''Thalamic stereotaxis for chronic pain: ablative lesion or stimulation?,'' *Stereotact Funct Neurosurg.* **64**(1), 47–55 (1995).
7. J. D. Atkinson, L. D. Collins, G. Bertrand, T. M. Peters, G. B. Pike, and A. F. Sadikot, ''Optimal location of thalamotomy lesions for tremor associated with Parkinson disease: a probalistic analysis based on postoperative magnetic resonance imaging and an integrated digital atlas,'' *J. Neurosurg.* **96**, 854–866 (2002).
8. A. M. Lozano, W. D. Hutchison, and J. O. Dostrovsky, ''Microelectrode monitoring of cortical and subcortical structures during stereotactic surgery,'' *Acta Neurochir. Suppl. (Wien)* **64**, 30–34 (1995).
9. J. K. Krauss, J. M. Desaloms, E. C. Lai, D. E. King, J. Jankovic, and R. G. Grossman, ''Microelectrode-guided posteroventral pallidotomy for treatment of Parkinson's disease: postoperative magnetic resonance imaging analysis,'' *J. Neurosurg.* **87**(3), 358–367 (1997).
10. T. Wichmann and M. R. DeLong, ''Models of basal ganglia function and pathophysiology of movement disorders,'' *Neurosurg Clin. N. Am.* **9**(2), 223–236 (1998).
11. O. Eriksson, K. Wårdell, N. E. Bylund, G. Kullberg, and S. Rehncrona, ''*In vitro* evaluation of brain lesioning electrodes (Leksell) using a computer-assisted video system,'' *Neurol. Res.* **21**(1), 89–95 (1999).
12. O. Eriksson and K. Wårdell, ''*In-vitro* size estimation of protein clots generated by brain electrodes,'' presented at Proceedings to the 20th Annual International Conference of the IEEE Engineering in Medicine and Biology Society, Hong Kong (1998).
13. O. Eriksson, E. O. Backlund, P. Lundberg, H. Lindstam, S. Lindström, and K. Wårdell, ''Experimental radiofrequency brain lesions: a volumetric study,'' *Neurosurgery* **51**(3), 781–787 (2002); **51**, 787–788 (2002).
14. E. R. Cosman, ''Radiofrequency lesions,'' in *Textbook of Stereotactic and Functional Neurosurgery*, P. L. Gildenberg and R. R. Tasker, Eds., pp. 973–975, McGraw-Hill, New York (1998).
15. J. Y. Lim and A. A. De Salles, ''Sequential postoperative appearance of radiofrequency pallidotomy lesions on MRI,'' *Stereotact Funct Neurosurg.* **69**(1–4), 46–53 (1997).
16. Y. Mamata, H. Mamata, A. Nabavi, D. F. Kacher, R. S. Pergolizzi, Jr., R. B. Schwartz, R. Kikinis, F. A. Jolesz, and S. E. Maier, ''Intraoperative diffusion imaging on a 0.5 Tesla interventional scanner,'' *J. Magn. Reson Imaging* **13**(1), 115–119 (2001).
17. K. H. Zou, S. K. Warfield, A. Bharatha, C. M. Tempany, M. R. Kaus, S. J. Haker, W. M. Wells III, F. A. Jolesz, and R. Kikinis, ''Statistical validation of image segmentation quality based on a spatial overlap index,'' *Acad. Radiol.* **11**(2), 178–189 (2004).
18. R. Steinmeier, J. Rachinger, M. Kaus, O. Ganslandt, W. Huk, and R. Fahlbusch, ''Factors influencing the application accuracy of neuronavigation systems,'' *Stereotact Funct Neurosurg.* **75**(4), 188–202 (2000).
19. A. P. Shepherd and P. Å. Öberg, *Laser-Doppler Blood Flowmetry*, Kluwer Academic, Dordrecht (1990).
20. G. E. Nilsson, E. G. Salerud, T. Strömberg, and K. Wårdell, ''Laser doppler perfusion monitoring and imaging,'' in *Biomedical Photonics Handbook*, T. Vo-Dinh, Ed., pp. 1–24, CRC Press, Cleveland (2003).
21. M. G. Karlsson, H. Casimir-Ahn, U. Lönn, and K. Wårdell, ''Analysis and processing of laser Doppler perfusion monitoring signals recorded from the beating heart,'' *Med. Biol. Eng. Comput.* **41**(3), 255–262 (2003).
22. A. Jakobsson and G. E. Nilsson, ''Prediction of sampling depth and photon pathlength in laser Doppler flowmetry,'' *Med. Biol. Eng. Comput.* **31**(3), 301–307 (1993).
23. A. Duncan, J. H. Meek, M. Clemence, C. E. Elwell, L. Tyszczuk, M. Cope, and D. T. Delpy, ''Optical pathlength measurements on adult head, calf and forearm and the head of the newborn infant using phase resolved optical spectroscopy,'' *Phys. Med. Biol.* **40**(2), 295–304 (1995).
24. M. Johns, C. A. Giller, and H. Liu, ''Computational and *in vivo* investigation of optical reflectance from human brain to assist neurosurgery,'' *J. Biomed. Opt.* **3**(4), 437–445 (1998).
25. Z. Qian, S. S. Victor, Y. Gu, C. A. Giller, and H. Liu, '''Look-ahead distance' of a fiber probe used to assist neurosurgery: phantom and Monte Carlo study,'' *Opt. Express* **11**(16), 1844–1855 (2003).